Bulk-edge correspondence with generalized chiral symmetry

Tohru Kawarabayashi [1] and Yasuhiro Hatsugai [2]
[1]*Department of Physics, Toho University, Funabashi 274-8510, Japan*
[2]*Department of Physics, University of Tsukuba, Tsukuba 305-8571, Japan*

(Received 24 November 2020; revised 1 April 2021; accepted 11 May 2021; published 24 May 2021)

The bulk-edge correspondence in topological phases is extended to systems with the generalized chiral symmetry, where the conventional chiral symmetry is broken. In such systems, we find that the edge state exhibits an unconventional behavior in the presence of the symmetry breaking by the mass, which is explored explicitly in the case of a deformed Su-Schrieffer-Heeger model. The localization length of the edge states diverges at a certain critical mass, where the edge state touches the bulk band. The edge state is specified by an imaginary wave vector that becomes real at the touching energy.

DOI: 10.1103/PhysRevB.103.205306

I. INTRODUCTION

Since the discovery of the topological insulators and superconductors [1,2], topological states of matter has been one of the central issues of the condensed matter physics. When the bulk topological invariant has a nontrivial value, the topological edge states emerge at the edges or boundaries of the system. This relationship between the bulk states and the edge states has been the hallmark of the topological phases of matter, which is called the bulk-edge correspondence originally introduced for the quantum Hall effect [3]. In classifying the topological phases, the chiral symmetry has been one of the important symmetries [4–7]. In particular, it has been shown that the chiral symmetry protects the zero-energy edge states at the boundary of the topological systems [8]. The concept of the bulk-edge correspondence in chiral symmetric systems has recently been extended to non-Hermitian systems [9,10].

Here in the present paper, we show that the bulk-edge correspondence can be extended to systems respecting an extension of the chiral symmetry, which we call the generalized chiral symmetry [11–13]. This can be achieved by the algebraic deformation of the chiral symmetric Hamiltonian in which the generalized chiral symmetry, introduced originally for the characterization of the tilted Dirac fermions in two dimensions [14–20], is always preserved. The deformation can be performed exactly in lattice models as well as in continuum models. The key ingredient is that the number of zero modes is an invariant of the deformation and this fact has enabled us to extend the topological protection of the doubling of the massless Dirac fermions on two-dimensional lattice models, which is understood as a consequence of the chiral symmetry [21–23], to the tilted Dirac fermions on a lattice model respecting the generalized chiral symmetry [24]. In the deformed systems, we find that the edge state shows an instability against the symmetry breaking by the mass. This is in sharp contrast to the case with the conventional chiral symmetry where the edge state is always robust against the symmetry breaking by the mass. This unconventional behavior of the edge state is explored in detail for the one-dimensional Su-Schrieffer-Heeger model.

The one-dimensional Su-Schrieffer-Heeger (SSH) model [25], introduced for analyzing the soliton state of polyacetylene, is a simple tight-binding model with a bond alternation induced by the electron-lattice coupling. Fundamental physical phenomena such as topological excitations in one dimension as well as the charge fractionalization associated with them [26–31] have been investigated based on the SSH model. It has served further as a prototypical model for illustrating the bulk-edge correspondence in the presence of the chiral symmetry [8–10]. In the recent progress of the experimental technique, the SSH model itself has been realized in an atom-optical system as well as in engineered atomic chains where the topological state has been experimentally confirmed [32–34].

The paper is organized as follows. We introduce, in Sec. II, the general theoretical frame work for the generalized chiral symmetry and the effect of the symmetry breaking by the mass. In Sec. III, we explore the unusual bulk-edge correspondence with the generalized chiral symmetry for deformed Su-Schrieffer-Heeger models. Section IV is devoted to the summary.

II. GENERAL FORMALISM

A. Generalized chiral symmetry

To discuss the bulk-edge correspondence in the topological phases, we consider systems with edges or boundaries. The algebraic deformation for generating a series of systems with the generalized chiral symmetry can be generally applicable to such systems with edges or boundaries [13]. The generalized chiral symmetry exists when the Hamiltonian H satisfies

$$\gamma^{\dagger} H \gamma = -H,$$

with $\gamma^2 = 1$, where the generalized chiral operator γ is not necessarily Hermitian [11,12]. The generalized chiral symmetry is an extension of the conventional chiral symmetry

since it reduces to the conventional one when the operator γ is Hermitian. The generalized chiral symmetry can be defined exactly for lattice Hamiltonians as well as for effective low-energy Hamiltonians [13].

To be specific, we consider the case where the original lattice Hamiltonian is bipartite. A bipartite Hamiltonian can generally be expressed as

$$H_{\rm c} = \begin{pmatrix} O & D \\ D^\dagger & O \end{pmatrix},$$

in a basis $(\Psi_{a_1}, \ldots, \Psi_{a_N}, \Psi_{b_1}, \ldots, \Psi_{b_N})$ where $\Psi_{a_n\ (b_n)}$ denotes the basis of the A (B) sublattice in the nth unit cell. Here D is a $N \times N$ matrix and N denotes the number of unit cells in the system. In this case, the conventional chiral operator is given by

$$\Gamma = \begin{pmatrix} I_N & O \\ O & -I_N \end{pmatrix} = \sigma_z \otimes I_N,$$

since it satisfies the relation $\Gamma H_{\rm c} \Gamma = -H_{\rm c}$ and $\Gamma^2 = 1$. Here I_N stands for the $N \times N$ identity matrix. The series of lattice Hamiltonians $H_\tau(q)$ respecting the generalized chiral symmetry can be generated from the chiral symmetric lattice Hamiltonian $H_{\rm c}$ by the algebraic transformation as

$$H_\tau(q) = T_\tau(q)^{-1} H_{\rm c} T_\tau(q)^{-1} \tag{1}$$

with

$$T_\tau(q) = \exp(q\boldsymbol{\tau} \cdot \boldsymbol{\sigma}/2) \otimes I_N,$$

where $\boldsymbol{\tau} = (\tau_x, \tau_y, \tau_z)$ is a three-dimensional real and unit vector and $\boldsymbol{\sigma} = (\sigma_x, \sigma_y, \sigma_z)$ are Pauli matrices. The parameter q is assumed to be real and thus $T_\tau(q)$ is an Hermitian matrix with $\det T_\tau(q) = 1$. We then define the generalized chiral operator γ as

$$\gamma = T_\tau(q) \Gamma T_\tau(q)^{-1}.$$

It is straightforward to see that $\gamma^2 = 1$ and $\gamma^\dagger H_\tau(q) \gamma = -H_\tau(q)$. The Hamiltonians deformed by the transformation (1) therefore always respect the generalized chiral symmetry. This hyperbolic transformation has the same form as the Lorentz boost (Appendix A).

Inversely, if we require the generalized chiral symmetry for a lattice model with the bipartite structure, it has been shown that the lattice model can be transformed back to a chiral symmetric lattice model [24]. For the case of 2×2 matrices, a matrix γ_2 satisfying $\gamma_2^2 = 1$ can be expressed in the form

$$\gamma_2 = \exp(q\boldsymbol{n}_1 \cdot \boldsymbol{\sigma}/2)(\boldsymbol{n}_0 \cdot \boldsymbol{\sigma}) \exp(-q\boldsymbol{n}_1 \cdot \boldsymbol{\sigma}/2),$$

where $\boldsymbol{n}_0$ and $\boldsymbol{n}_1$ are real vectors with $\boldsymbol{n}_0^2 = \boldsymbol{n}_1^2 = 1$ and $\boldsymbol{n}_0 \cdot \boldsymbol{n}_1 = 0$. The generalized chiral operator γ_s can thus be expressed generally in the real space as

$$\gamma_s = \gamma_2 \otimes I_N = S_{n_1}(q) \Gamma' S_{n_1}(q)^{-1}$$

with

$$S_{n_1}(q) = \exp(q\boldsymbol{n}_1 \cdot \boldsymbol{\sigma}/2) \otimes I_N, \quad \Gamma' = (\boldsymbol{n}_0 \cdot \boldsymbol{\sigma}) \otimes I_N.$$

When the Hamiltonian H respects the generalized chiral symmetry as $\gamma_s^\dagger H \gamma_s = -H$, we can then define an inverse transformation as

$$H_{\rm c}' = S_n(q) H S_n(q). \tag{2}$$

It is then verified that $H_{\rm c}'$ is indeed chiral symmetric, because it satisfies the relation $\Gamma' H_{\rm c}' \Gamma' = -H_{\rm c}'$ with $\Gamma' = (\boldsymbol{n}_0 \cdot \boldsymbol{\sigma})$ and $(\Gamma')^2 = 1$.

It should be noted that the number of zero-energy states is an invariant of the transformation and its inverse. If we have a zero-energy state ψ_0, for instance, of the original Hamiltonian $H_{\rm c}$, namely, $H_{\rm c}\psi_0 = 0$, then it is easy to see that the state defined by $T_\tau(q)\psi_0$ is also a zero-energy state of $H_\tau(q)$ since $H_\tau(q)[T_\tau(q)\psi_0] = T_\tau(q)^{-1} H_{\rm c} \psi_0 = 0$. Taking into account that $\det T_\tau(q) = 1$, we can safely conclude that the number of zero-energy states is an invariant of the deformation.

If the original system $H_{\rm c}$ is topologically nontrivial, we have the topological edge states at the open boundary of the system, which are the zero-energy states because of the chiral symmetry. It is to be remarked, however, that the energy of the edge state localized at the boundary becomes exactly zero only in the thermodynamic limit ($N \to \infty$) where the mixing between edge states at both boundaries becomes negligible. In a conventional approach, therefore, a semi-infinite system with one boundary has been considered to define the edge states as the zero-energy states. Here in the present paper, we adopt an alternative approach to define the edge states based on the exact zero-energy states for a finite system ($N < \infty$).

Instead of a semi-infinite system, we consider simply a finite system ($N < 0$) having the left and the right boundaries at both ends of the system. To define the edge state, for example, at the left boundary, we first modify the Hamiltonian at the right end of the system so that there exist exact zero-energy states even for a finite N. This can be achieved rather easily as we demonstrate for the SSH model in Sec. III. We then take the thermodynamic limit $N \to \infty$ where one of the zero modes becomes the edge state at the left boundary. It is to be noted that, in the thermodynamic limit, the local modification of the Hamiltonian in the vicinity of one end of the system should be negligible for the edge state localized at the other end. Though this approach gives the same result as the conventional one, it has an advantage that we can safely assume the existence of the exact zero-energy states even in the present real-space formalism where the system is described by a large but finite-size matrix.

In numerical analyses for finite systems, the deviation of the energy of the edge state from zero should be exponentially small and thus can be negligible when the system size (N) is much larger than the localization length of the edge state.

Since the deformation preserves the number of zero modes, the number of edge states is also an invariant of the deformation. This clearly suggests that the bulk topological invariant should also be preserved within the present deformation. This property of the deformation also leads to the fact that if the original chiral symmetric model has an energy gap in the bulk spectrum, it remains open and never closes in any deformed models with arbitrary q. Note that because of the chiral symmetry, if the gap exists, it should be open symmetrically around zero energy ($E = 0$) in the original model. In the deformed Hamiltonian generated by the transformation (1), the zero-energy states should never appear in the bulk

spectrum and the positive/negative energy states should remain positive/negative for any q.

B. Symmetry breaking

Let us discuss the effect of the symmetry breaking by the mass term

$$H_m = m\Gamma.$$

To be specific, we assume m is positive. We find that the robustness of the edge states against the mass term for $q \neq 0$ turns out to be quite different from that for $q = 0$. To see this, it is instructive to revisit the robustness of the edge state for $q = 0$. In this case, the Hamiltonian is chiral symmetric for $m = 0$, and therefore the zero-energy edge states can be expressed as an eigenstate of the chiral operator. This leads to the fact that the energies of the edge states are exactly given by $E_{\rm edge}(m) = \pm m$ and the corresponding eigenstates are independent of m. The edge state localized at the boundary therefore never disappears for any value of m.

For deformed systems ($q \neq 0$), the behavior of the edge states in the presence of the mass term is qualitatively different. Let us recall the general theoretical framework [13] for the energy eigenvalues of deformed systems with the generalized chiral symmetry. To discuss systems with open boundaries, we proceed to the real-space representation in a basis $(\Psi_{a_1}, \ldots, \Psi_{a_N}, \Psi_{b_1}, \ldots, \Psi_{b_N})$. The deformed Hamiltonian in the presence of the mass term is then defined by

$$H_\tau^{(m)}(q) = T_\tau(q)^{-1}(H_{\rm c} + m\Gamma)T_\tau(q)^{-1}.$$

Since the operator $T_\tau(q)$ with $\boldsymbol{\tau} = (0, 0, 1)$ induces no changes for $H_{\rm c}$, we confine ourselves to the case $\boldsymbol{\tau} = (\cos\theta, \sin\theta, 0)$. We then have

$$H_\tau^{(m)}(q) = H_\tau(q) + m\Gamma$$

since we have a relation $\Gamma T_\tau(q) = T_\tau(-q)\Gamma$. Eigenvalue equations are given by

$$H_\tau^{(m)}(q)\psi_E^{(m)} = E\psi_E^{(m)},$$

where E depends on m. Multiplying $H_\tau^{(m)}(-q) = H_\tau^{(m)}(q) + I_2 \otimes (e^{i\theta}D + e^{-i\theta}D^\dagger)\sinh q$, we have [13]

$$\begin{aligned} &H_\tau^{(m)}(-q)H_\tau^{(m)}(q)\psi_E^{(m)} \\ &= T_\tau(q)\big(H_{\rm c}^2 + m^2\big)T_\tau(q)^{-1}\psi_E^{(m)} \\ &= E[E + I_2 \otimes (e^{i\theta}D + e^{-i\theta}D^\dagger)\sinh q]\psi_E^{(m)}, \end{aligned}$$

which leads to

$$\big[H_{\rm c}^2 - I_2 \otimes E(e^{i\theta}D + e^{-i\theta}D^\dagger)\sinh q + m^2\big]\Phi_E^{(m)} = E^2\Phi_E^{(m)}$$

with $\Phi_E^{(m)} = T_\tau(q)^{-1}\psi_E^{(m)}$. Completing the square, we have

$$\big\{[H_{\rm c}(q, E)]^2 + m_R^2\big\}\Phi_E^{(m)} = E^2\Phi_E^{(m)}$$

with

$$H_{\rm c}(q, E) = \begin{pmatrix} O & D(q, E) \\ D^\dagger(q, E) & O \end{pmatrix},$$

$$D(q, E) \equiv \frac{1}{\cosh q}(D - e^{-i\theta}E\sinh q)$$

and $m_R \equiv m/\cosh q$. We have therefore generally $E^2 \geqslant m_R^2$. The condition under which the eigenstate with an eigenvalue $E = m_R$ in the form

$$\psi_{E=m_R}^{(m)} = T_\tau(q)\begin{pmatrix} \phi_+^m \\ 0 \end{pmatrix} \tag{3}$$

exists, is given by [13]

$$(D^\dagger - m_R e^{i\theta}\sinh q)\phi_+^m = 0. \tag{4}$$

For the eigenstate $\psi_{E=-m_R}$ with the energy $E = -m_R$ in the form

$$\psi_{E=-m_R}^{(m)} = T_\tau(q)\begin{pmatrix} 0 \\ \phi_-^m \end{pmatrix}, \tag{5}$$

the condition is similarly given by

$$(D + m_R e^{-i\theta}\sinh q)\phi_-^m = 0. \tag{6}$$

Note that the eigenstate $\psi_{E=\pm m_R}^{(m)}$, if it exists, is also the eigenstate of the generalized chiral operator γ with the eigenvalue ± 1 and reduces to the eigenstate of the conventional chiral operator Γ in the limit as $q \to 0$.

The state $\psi_{E=\pm m_R}^{(m)}$ with the energy $\pm m_R$ is apparently a candidate for the edge state of the topological system because it is connected to the zero mode in the bulk gap in the limit as $m \to 0$. We therefore look for an eigenstate with $E = \pm m_R$ with the form $\psi_{E=\pm m_R}^{(m)}$ decaying exponentially from one end of the system to the other. To discuss such a state localized at one end of the system, it is allowed to modify the original Hamiltonian locally at the other end of the system, since the amplitude of the state is exponentially small there and the effect of the modification should be negligible in the thermodynamic limit. The modification to obtain, for instance, an exact eigenstate $\psi_{E=m_R}^{(m)}$ is performed so that the above condition (4) is satisfied by a nonzero solution ϕ_+^m even for a finite system. This can be achieved, practically, by a modification that reduces the rank of the matrix $(D^\dagger - m_R e^{i\theta}\sinh q)$ from N to $N - 1$. Though such a modification certainly depends on the details of the Hamiltonian, it is realized generally as long as it is composed of local operators. With this modification, we can construct an exact eigenstate $\psi_{E=\pm m_R}^{(m)}$ decaying exponentially from one end to the other even for a finite N, with which we define the edge state in the limit as $N \to \infty$.

Exponentially decaying states can be understood as plane waves with complex wave numbers. If we adopt the expression $\phi_\pm^m[j] = e^{ikr_j}u_{\pm,j}^m(k)$ with $u_{\pm,j}^m(k) = u_{\pm,j+\alpha}^m(k)$ where r_j denotes the spatial coordinate of the site j, which is assumed to increase from left to right, and α is the number of the A (B) site in the unit cell. The condition (4) for the state $\psi_{E=m_R}^{(m)}$ then can be expressed as

$$[d^\dagger(k) - m_R e^{i\theta}\sinh q]u_+^m(k) = 0,$$

where $d(k)$ is a complex matrix in the Hamiltonian expressed in the momentum space as

$$H_{\rm c}(k) = \begin{pmatrix} 0 & d(k) \\ d^\dagger(k) & 0 \end{pmatrix},$$

and $u_+^m(k) = {}^t[u_{+,1}^m(k), \ldots, u_{+,\alpha}^m(k)]$. Note that $d(k)$ is a matrix for a multiband system

($\alpha > 1$). The wave number k is therefore determined by

$$\det[d(k)^\dagger - m_R e^{-i\theta}\sinh q] = 0.$$

Similarly, for the state $\psi^{(m)}_{E=-m_R}$, the condition (6) becomes $[d(k) + m_R e^{-i\theta}\sinh q]u^m_-(k) = 0$. The momentum k is then determined by $\det[d(k) + m_R e^{-i\theta}\sinh q] = 0$.

When the above equations have a solution with a wave number k with a nonzero imaginary part, $\mathrm{Im}(k) \neq 0$, the solution is an exponentially decaying (diverging) state which corresponds to the edge state localized at the left (right) boundary of a semi-infinite system. The imaginary part of k must be positive (negative) for an edge state localized at the left (right) boundary, so that the edge states are normalizable. In general, the behavior of the imaginary part of k as a function of the mass m determines the instability of the edge state. If $\mathrm{Im}(k)$ becomes zero at a certain value m_c of the mass, the edge state at $m = m_c$ is no longer localized at one boundary of the system and is expected to become a bulk state.

As we shall see in the following, for the case of the one-dimensional SSH model with $\alpha = 1$, these eigenstates $\psi_{E=\pm m_R}$ are indeed the edge states exponentially localized at the boundaries of the system in the presence of the mass term, where the sign of the imaginary part of the wave number determines the position of the edge state (left or right boundaries). It is clearly demonstrated that they merge into the bulk band and disappear at a certain critical mass where the imaginary part of the wave vector k becomes exactly zero.

III. DEFORMED SSH MODEL

A. Topological invariant and edge states

Here we consider deformations of the one-dimensional SSH model [25], which is described by the Hamiltonian

$$H_{\mathrm{SSH}} = \sum_n t a_n^\dagger b_n + t' a_{n+1}^\dagger b_n + \mathrm{H.c.},$$

where a_n (b_n) denotes the annihilation operator of an electron on the sublattice A (B) in the nth unit cell (Fig. 1). This Hamiltonian respects the chiral symmetry and can be expressed as

$$H_{\mathrm{SSH}} = \begin{pmatrix} 0 & D \\ D^\dagger & 0 \end{pmatrix}$$

in the basis $(\Psi_{a_1}, \ldots, \Psi_{a_N}, \Psi_{b_1}, \ldots, \Psi_{b_N})$ where the nonzero matrix elements of the off-diagonal matrix D are given by $D_{i,i} = t$ for $i = 1, \ldots, N$ and $D_{i+1,i} = t'$ for $i = 1, \ldots, N-1$. The symmetry breaking mass term is defined by

$$H_m = m\Gamma = m\sum_{n=1}^{N}(a_n^\dagger a_n - b_n^\dagger b_n).$$

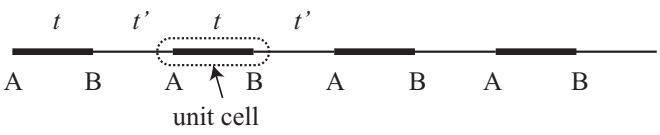

FIG. 1. The SSH model in real space. The transfer integral in the unit cell is denoted by t and that between the unit cells is denoted by t'.

In the momentum space, the bulk Hamiltonian with the mass term can be expressed as

$$H_{\mathrm{SSH}}(k) + m\sigma_z = \begin{pmatrix} m & d(k) \\ d^*(k) & -m \end{pmatrix},$$

with $d(k) = t + t'e^{-ik}$. Here we adopt the lattice constant as a unit of length. The bulk energy dispersion is therefore given by

$$E(k) = \pm\sqrt{|d(k)|^2 + m^2}.$$

For $m = 0$, this model becomes topologically nontrivial when $t' > t$ exhibiting topological edge states at $E = 0$ if the system has open boundaries, while it is trivial when $t' < t$ having no edge state at the open boundary [7,8]. In the presence of the mass, the wave function of the edge states remains the same as that for $m = 0$ while their energies become $\pm m$. The edge state with the conventional chiral symmetry therefore never goes into the bulk band since $E(k)^2 > m^2$ as long as $|d(k)| > 0$, nor disappears at a certain finite value of the mass because the wave function itself is independent of m.

The deformed SSH model is defined by the algebraic transformation

$$H_\tau(q) = T_\tau(q)^{-1} H_{\mathrm{SSH}} T_\tau(q)^{-1}$$

with $\boldsymbol{\tau} = (\cos\theta, \sin\theta, 0)$, which can be represented generally as [13]

$$H_\tau(q) = -\frac{\sinh q}{2}(e^{i\theta}D + e^{-i\theta}D^\dagger) \otimes I_2 + \begin{pmatrix} O & D_q \\ D_q^\dagger & O \end{pmatrix}$$

with

$$D_q \equiv D\cosh^2\frac{q}{2} + e^{-2i\theta}D^\dagger\sinh^2\frac{q}{2}.$$

The present deformation of the Hamiltonian in real space can be applied to systems with boundaries. The deformation preserves the number of zero-energy states and therefore preserves the number of edge states of the topological phase in the original SSH model. The deformed system is thus topologically nontrivial and has edge states for the case of $t' > t$.

This can be confirmed by evaluating the bulk topological invariant in the system with the translational invariance. In such a system, the deformed Hamiltonian can be given in the momentum space as

$$H_\tau(q) = -\sinh q\,\mathrm{Re}[e^{i\theta}d(k)]I_2 + \begin{pmatrix} 0 & d_{q,\theta}(k) \\ d^*_{q,\theta}(k) & 0 \end{pmatrix}$$

with $d_{q,\theta}(k) = e^{-i\theta}\{\mathrm{Re}[e^{i\theta}d(k)]\cosh q + i\,\mathrm{Im}[e^{i\theta}d(k)]\}$ where Re (Im)[z] stands for the real (imaginary) part of a complex number z. With this expression, it is straightforward to verify that the winding number, which is the topological invariant of the topological phase of the SSH model [5,8], is indeed an invariant of the deformation (see Appendix B). In real space, the deformed system can be realized as a ladder system with the next-nearest neighbor transfer integrals which exhibits various types of band structure including a flatband as well as an indirect band gap (Appendix C).

Now let us discuss the symmetry breaking in the deformed systems. The deformed SSH model with the mass term is

given by

$$H_\tau^{(m)}(q) \equiv T_\tau(q)^{-1}(H_{\rm SSH} + m\Gamma)T_\tau(q)^{-1} = H_\tau(q) + m\Gamma.$$

To discuss the edge states, we consider a finite system with N unit cells having an A site at its left boundary (Fig. 1) and examine whether the state with the form $\psi^{(m)}_{E=m_R}$ can describe the edge state at the left boundary decaying exponentially toward the right [$\mathrm{Im}(k) > 0$]. For the SSH model, condition (4) can be written explicitly as

$$(t - m_R e^{i\theta}\sinh q)\phi^m_+[n] + t'\phi^m_+[n+1] = 0,$$

for $n = 1, 2, \ldots, N-1$, with

$$(t - m_R e^{i\theta}\sinh q)\phi^m_+[N] = 0 \tag{7}$$

at the right boundary. Here the element of the nth unit cell is denoted by $\phi^m_+[n]$ so that $\phi^m_+ = {}^t(\phi^m_+[1], \phi^m_+[2], \ldots, \phi^m_+[N])$. The index n for the nth unit cell is assumed to increase from left to right where the unit cell at the left boundary is denoted by $n = 1$. For a finite N, no physical solution is allowed due to condition (7), suggesting that the edge state having exactly the energy $E = m_R$ does not exist in a finite system.

We then perform a modification of $H_{\rm SSH}$ at the right boundary of the system to define a modified Hamiltonian $\tilde{H}^+_{\rm SSH}$ as

$$\tilde{H}^+_{\rm SSH} = H_{\rm SSH} + \{(m_R e^{-i\theta}\sinh q - t)a^\dagger_N b_N + \mathrm{H.c.}\},$$

so that the coefficient of $\phi^m_+[N]$ in (7) vanishes. This modification is nothing but the replacement of the local Hamiltonian $\{ta^\dagger_N b_N + \mathrm{H.c.}\}$ with $\{(m_R e^{-i\theta}\sinh q)a^\dagger_N b_N + \mathrm{H.c.}\}$ at the Nth unit cell. With this modification at the right boundary, the (N, N) element of the matrix $\tilde{D}$ defined as

$$\tilde{H}^+_{\rm SSH} = \begin{pmatrix} O & \tilde{D} \\ \tilde{D}^\dagger & O \end{pmatrix}$$

becomes $\tilde{D}_{N,N} = (m_R e^{-i\theta}\sinh q)$, while other elements of $\tilde{D}$ are the same as D. Note that the modification affects only the (N, N) element of the matrix D. It is then easy to verify that the rank of the matrix $[\tilde{D}^\dagger - m_R e^{i\theta}\sinh q]$ is reduced to $N-1$ and hence the nonzero solution with the energy m_R can exist even for a finite N. More explicitly, the equations become

$$(t - m_R e^{i\theta}\sinh q)\tilde{\phi}^m_+[n] + t'\tilde{\phi}^m_+[n+1] = 0,$$

for $n = 1, \ldots, N-1$, with which the eigenstate $\tilde{\psi}^{(m)}_{E=m_R}$ with the energy $E = m_R$ for $\tilde{H}^+_{\rm SSH}$ is given by

$$\tilde{\psi}^{(m)}_{E=m_R} = T(q)\begin{pmatrix} \tilde{\phi}^m_+ \\ 0 \end{pmatrix}.$$

Note that the equations for $\tilde{\phi}^m_+$ are exactly the same as those for ϕ^m_+ except the condition (7).

For the modified system, we can construct a nonzero solution decaying (diverging) exponentially from the left boundary to the bulk even for a finite system as $\tilde{\phi}^m_+[n] \propto (-1)^{n-1} r_+^{n-1}$ with

$$r_+ \equiv \frac{t - m_R e^{i\theta}\sinh q}{t'}.$$

Note that the energy of the state is exactly given by m_R even for a finite system. We then consider the thermodynamic limit as $N \to \infty$, where the state is normalizable and decaying exponentially as long as $|r_+| < 1$ is satisfied. It is again remarked that, in the limit as $N \to \infty$, the effect of the modification at the right end of the system should be negligible for the edge state localized at the left boundary. We therefore remove the tilde in the notations and arrive at the solution for the edge state at the left boundary

$$\psi^{(m)}_{E=m_R} = \begin{pmatrix} \psi^m_{+,A} \\ \psi^m_{+,B} \end{pmatrix}$$

with

$$\psi^m_{+,A}[n] = (-1)^{n-1} C_+ \cosh(q/2) r_+^{n-1},$$
$$\psi^m_{+,B}[n] = (-1)^{n-1} C_+ e^{i\theta}\sinh(q/2) r_+^{n-1},$$

where $\psi^m_{+,A\ (B)}[n]$ denotes the element of $\psi^m_{+,A\ (B)}$ at the unit cell specified by the index n and

$$C_+ = \left(\frac{1 - |r_+|^2}{\cosh q}\right)^{1/2}$$

is a normalization constant. This normalizable eigenstate reduces to the conventional edge state at the left end of the system in the limit as $q \to 0$ which resides only on the A sublattice.

The present approach to define the edge state also indicates that the state $\psi^{(m)}_{E=m_R}$ with the energy m_R is inappropriate for the edge state at the right boundary, which should decay exponentially from right to left [$\mathrm{Im}(k) < 0$]. Apparently, condition (7) cannot be removed by the local modification of the Hamiltonian at the left end of the system. We are therefore unable to construct a nonzero solution decaying from the right boundary to the left by assuming the form $\psi^{(m)}_{E=m_R}$, suggesting that the state with the energy m_R does not exist in the regime $\mathrm{Im}(k) < 0$.

To consider the edge states at the right boundary decaying exponentially toward the bulk, we examine the state $\psi^{(m)}_{E=-m_R}$ having the energy $-m_R$. With our choice of the unit cell, we have a B site at the right boundary. In such a case, condition (6) for the eigenstate $\psi^{(m)}_{E=-m_R}$ can be written, using the elements of $\phi^m_- = {}^t(\phi^m_-[1], \ldots, \phi^m_-[N])$, as

$$(t + m_R e^{-i\theta}\sinh q)\phi^m_-[n] + t'\phi^m_-[n-1] = 0,$$

for $n = 2, \ldots, N$ with

$$(t + m_R e^{-i\theta}\sinh q)\phi^m_-[1] = 0 \tag{8}$$

at the left boundary. A nonzero solution is again prohibited by condition (8) for a finite system ($N < \infty$).

We then consider again a similar local modification of the Hamiltonian at the opposite (left) end of the system so that the coefficient of $\phi^m[1]$ in condition (8) becomes zero. It is achieved by modifying the local Hamiltonian in the first cell ($n = 1$) at the left end of the system as

$$\tilde{H}^-_{\rm SSH} = H_{\rm SSH} - \{(m_R e^{-i\theta}\sinh q + t)a^\dagger_1 b_1 + \mathrm{H.c.}\}.$$

If we write the eigenstate $\tilde{\psi}^{(m)}_{E=-m_R}$ of the modified Hamiltonian $\tilde{H}^-_{\rm SSH}$ with the energy $-m_R$ as

$$\tilde{\psi}^{(m)}_{E=-m_R} = T(q)\begin{pmatrix} 0 \\ \tilde{\phi}^m_- \end{pmatrix},$$

the equations for $\tilde{\phi}^m_-$ becomes

$$(t + m_R e^{-i\theta} \sinh q)\tilde{\phi}^m_-[n] + t'\tilde{\phi}^m_-[n-1] = 0,$$

for $n = 2, \ldots, N$, which are exactly the same as those for ϕ^m_- except the condition (8).

We are then able to construct a solution that decays exponentially from the right edge to the bulk as $\phi^m_-[n] \propto (-1)^{N-n} r_-^{N-n}$ with

$$r_- \equiv \frac{t + m_R e^{-i\theta} \sinh q}{t'},$$

which is normalizable in the limit as $N \to \infty$ provided that $|r_-| < 1$. The edge state at the right boundary is thus given by

$$\psi^{(m)}_{E=-m_R} = \begin{pmatrix} \psi^m_{-,A} \\ \psi^m_{-,B} \end{pmatrix}$$

with

$$\psi^m_{-,A}[n] = (-1)^{N-n} C_- \cosh(q/2) r_-^{N-n},$$
$$\psi^m_{-,B}[n] = (-1)^{N-n} C_- e^{i\theta} \sinh(q/2) r_-^{N-n}.$$

Here $\psi^m_{-,A(B)}[n]$ denotes the element of $\psi^m_{-,A(B)}$ at the nth unit cell and

$$C_- = \left(\frac{1 - |r_-|^2}{\cosh q}\right)^{1/2}$$

is again a normalization constant. This solution reduces to the conventional edge state at the right boundary in the limit as $q \to 0$ which resides only on the B sublattice.

It is also noted that the state $\psi^{(m)}_{E=-m_R}$ with the energy $-m_R$ cannot describe the edge state at the left boundary decaying from left to right [$\mathrm{Im}(k) > 0$], because we cannot remove condition (8) by a local modification of the Hamiltonian at the right boundary.

The eigenstates with energies $E = \pm m_R$ are therefore indeed the edge states exponentially localized at the boundaries of the deformed system. These edge states exist only when the mass is smaller than the critical mass $m_c^{\pm}$ determined by $|r_\pm| = 1$ so that condition $|r_\pm| < 1$ is satisfied for $m < m_c^{\pm}$.

It is to be noted that $|r_+|$ and $|r_-|$ can be different, which means that the robustness of the edge state with the energy $E = m_R$ and that with $E = -m_R$ can be different for a deformed system. As we shall see in the following, the edge state merges into the bulk band at a point where $|r_+|$ ($|r_-|$) becomes unity.

Here we explicitly construct the edge state based on the boundary condition and its normalizability in a semi-infinite system. We note that the edge states with generic boundary conditions have been discussed for continuum models [35–37].

B. Bulk versus edge states

As shown above, the edge state exhibits an instability at $|r_\pm| = 1$. This condition can be understood as the point where the wave number of the plane-wave solution with the energy $\pm m_R$ becomes real, which means that the edge state becomes one of the bulk states exactly at this point. This is the reason why the edge state merges into the bulk band at $|r_\pm| = 1$.

If we adopt the form $\phi^m_\pm[n] = e^{ikn}u(k)$, the conditions (4) and (6) for the states $\psi^{(m)}_{E=\pm m_R}$ are expressed as

$$(t + t'e^{\pm ik}) \mp m_R e^{\pm i\theta} \sinh q = 0.$$

For $q = 0$, this reduces to $t + t'e^{\pm ik} = 0$ and the wave number k is $k = \mp i \ln(-t/t')$. In the topological phase ($t' > t$), the imaginary part of k is positive [$\mathrm{Im}(k) > 0$] for the state $\psi^{(m)}_{E=m_R}$ which corresponds to an exponentially decaying state at the left boundary. For the state $\psi^{(m)}_{E=-m_R}$, we have $\mathrm{Im}(k) < 0$ which means that the state is exponentially decaying from right to left at the right boundary. Note that the wave number is always complex independent of m, which means that the edge state never merges into the bulk band.

For $q \neq 0$, on the other hand, the wave number k of the states with $E = \pm m_R$ is given as

$$e^{\pm ik} = -\frac{t \mp m_R e^{\pm i\theta} \sinh q}{t'},$$

and hence we have $e^{\pm ik} = -r_\pm$. The requirement that $|r_\pm| = 1$ is therefore equivalent to the condition that the wave vector k is real. At this point, the sign of the imaginary part of the wave number k changes from positive (negative) to negative (positive) for the state $\psi^{(m)}_{E=m_R}$ ($\psi^{(m)}_{E=-m_R}$), as the mass is increased. Since the state $\psi^{(m)}_{E=m_R}$ ($\psi^{(m)}_{E=-m_R}$) exists only as the left (right) edge state, it is normalizable and therefore exists only when the imaginary part of the wave number $\mathrm{Im}(k)$ is positive (negative). In the deformed system, therefore, the edge states

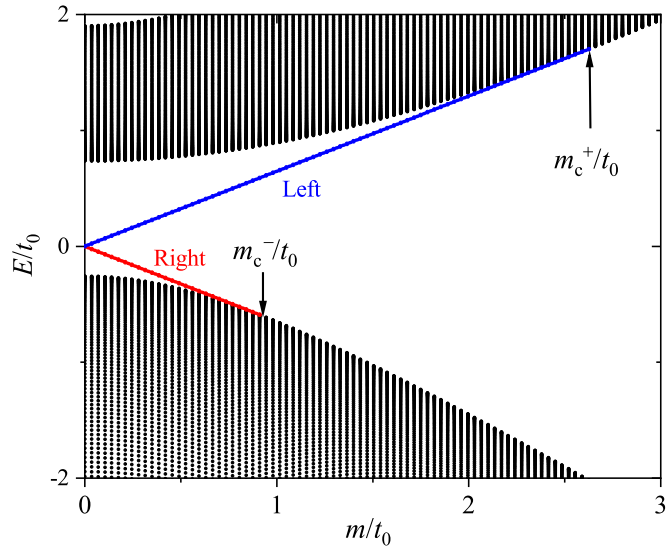

FIG. 2. Energy eigenvalues for a system in the case of $\theta = 0$ with the symmetry breaking term $m\Gamma$. The numerical results for a finite system with 200 unit cells having two open boundaries at each end of the system are shown. The parameters are assumed to be $t/t_0 = 0.65$, $t'/t_0 = 1.35$, and $q = 1.0$. The bulk states in the Bloch bands are plotted by black symbols while the two edge states with the energy $\pm m_R$ in the bulk gap are plotted by red ($-m_R$) and blue ($+m_R$) lines. It is clearly seen that the edge state at the left end (blue line) exists in the range $0 < m < (t' + t)/\tanh q$ and merges into the bulk band at $m_c^+ = (t' + t)/\tanh q \approx 2.6t_0$. The edge state at the right end (red line), on the other hand, merges into the bulk band at $m_c^- = (t' - t)/\tanh q \approx 0.9t_0$.

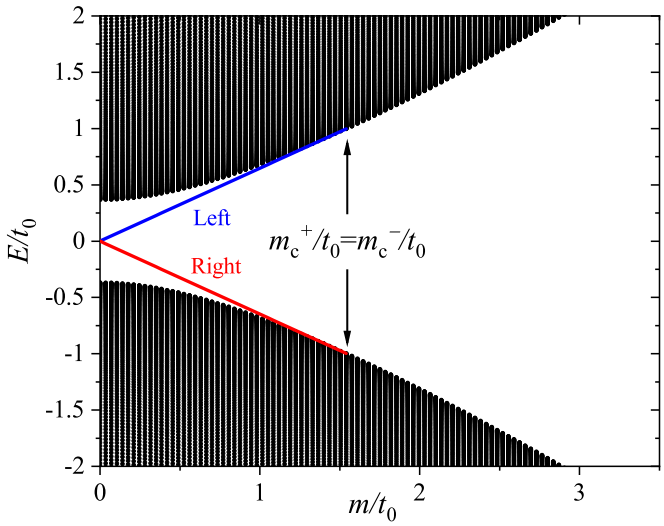

FIG. 3. Energy eigenvalues for a system in the case of $\theta = \pi/2$ with the symmetry breaking term $m\Gamma$. The numerical results for a finite system with 200 unit cells having two open boundaries at each end of the system is shown. The parameters are assumed to be $t/t_0 = 0.65$, $t'/t_0 = 1.35$, and $q = 1.0$. The bulk states in the Bloch bands are plotted by black symbols while the two edge states with the energy $\pm m_R$ are plotted by red $(-m_R)$ and blue $(+m_R)$ lines. It is clearly seen that both the edge states (blue and red lines) exist in the range $0 < m < \sqrt{t'^2 - t^2}/\tanh q$ and merges into the bulk band at $m_c^+ = m_c^- = \sqrt{t'^2 - t^2}/\tanh q \approx 1.55t_0$.

disappear at the critical mass $m_c^{\pm}$ where the imaginary part of k vanishes, and becomes a bulk state there, which does not happen in the conventional chiral symmetric systems.

C. Numerical results

To confirm the analytical results, we perform numerical calculations in systems with boundaries. First, we consider the case of $\theta = 0$, where the time-reversal symmetry (TRS) is preserved [13]. In this case, the edge state with $E = m_R$ exists as long as

$$|t - m\ \tanh q| < |t'|,$$

while the edge state with $E = -m_R$ exists when

$$|t + m\ \tanh q| < |t'|.$$

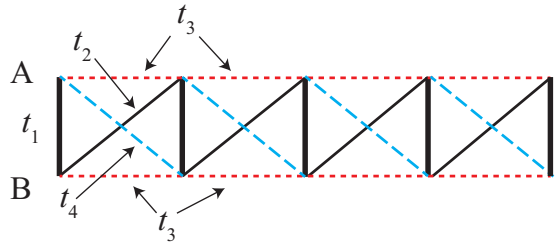

FIG. 4. The deformed SSH model with $\boldsymbol{\tau} = \hat{\boldsymbol{x}}$ in real space. Thick solid lines (black), thin solid lines (black), dotted lines (red), and dashed lines (blue) represent hopping amplitudes t_1, t_2, t_3, and t_4, respectively.

For the case where t, $t'(>t)$, and m are positive, these conditions lead to the fact that for $0 < m \tanh q < t' - t$ the edge states at both boundaries (left and right) exist in the gap while for $t' - t < m \tanh q < t + t'$ only the edge state at the left boundary can exist in the gap. The critical masses $m_c^{\pm}$ over which the edge state merges into the bulk band are given by $m_c^+ = (t + t')/\tanh q$ and $m_c^- = (t' - t)/\tanh q$. This can be clearly seen in Fig. 2 where the energy spectra for the deformed system $H_q^{\hat{x}} + m\Gamma$ with open boundaries are shown.

Next, we consider the case of $\theta = \pi/2$, where the time-reversal symmetry is broken. The critical mass $m_c^{\pm}$ is then given by $m_c^+ = m_c^- = \sqrt{t'^2 - t^2}/\tanh q$, and therefore both edge states exist only when the condition $m < m_c^{\pm}$ is satisfied (Fig. 3). In this case, the energy spectra are symmetric with respect to $E = 0$. Note that in both cases, no eigenstate with the energy $E = \pm m_R$ exists for $m > m_c^{\pm}$.

IV. SUMMARY

We have shown that the bulk-edge correspondence in topological phases can be extended to the systems without the conventional chiral symmetry but respecting the generalized chiral symmetry. Systems respecting the generalized chiral symmetry are generated by the algebraic deformation which preserves the bulk topological invariants of the original chiral symmetric system as well as the zero-energy edge states at the boundaries. We have explored the bulk-edge correspondence in a deformed Su-Schrieffer-Heeger model in one dimension. We have found interestingly that the edge states in a deformed system with generalized chiral symmetry exhibit an instability when the symmetry is broken by the mass. The edge state disappears at a certain critical value of the mass, where it touches to the bulk band and becomes a bulk state with a real wave number, which never happens for the conventional chiral symmetric systems. The present analysis suggests that in the bulk-edge correspondence with the generalized chiral symmetry, the edge states are adiabatically connected to the bulk states by modifying the strength of the symmetry breaking.

ACKNOWLEDGMENTS

The work was supported in part by JSPS KAKENHI Grants No. JP19K03660 (T.K.) and No. JP17H06138.

APPENDIX A: DEFORMATION AND LORENTZ BOOST

The present deformation has the same hyperbolic form as the Lorentz boost [38–41]. To see the relationship between them, we consider the two-dimensional massless Dirac electrons described by the effective Hamiltonian $H = v_F(\sigma_x p_x + \sigma_y p_y)$. Then the Schrödinger equation becomes

$$\left(i\hbar\frac{\partial}{\partial t} - H\right)\psi = 0.$$

This can be reduced to, in the real-space representation,

$$(\partial_0 + \sigma_x\partial_x + \sigma_y\partial_y)\psi = 0,$$

where $\partial_0 = \frac{\partial}{\partial x_0}$, $\partial_x = \frac{\partial}{\partial x}$, and $\partial_y = \frac{\partial}{\partial y}$ with $x_0 = v_F t$. We then consider a Lorentz boost for the frame moving in the

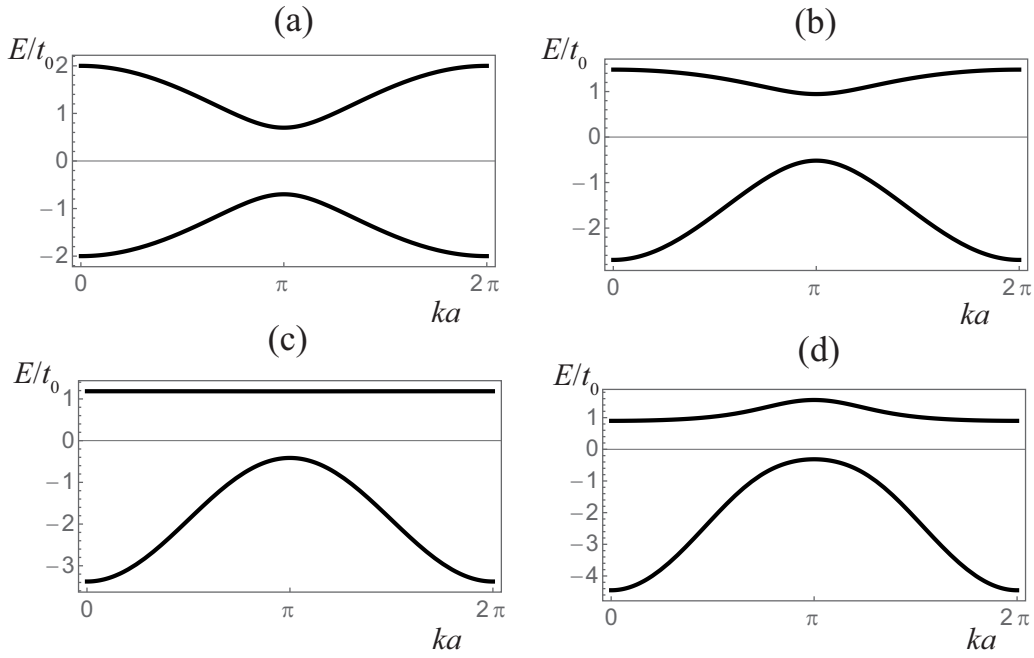

FIG. 5. Energy dispersions $E^{\hat{x}}_{q,\pm}$ of the deformed SSH model for (a) $q = 0$, (b) $q = 0.3$, (c) $q = \tanh^{-1}(t/t') \approx 0.524$, and (d) $q = 0.8$. Because of the time-reversal symmetry, we have $E^{\hat{x}}_{q,\pm}(k) = E^{\hat{x}}_{q,\pm}(-k)$. Here we assume $t = t_0 - \delta t$, $t' = t_0 + \delta t$ with $\delta t/t_0 = 0.35$ so that the original SSH model is topologically nontrivial. The lattice constant of the corresponding lattice is denoted by a. A flatband appears for the case of (c). For $q > \tanh^{-1}(t/t')$, the band gap becomes indirect (d).

x direction with a velocity v. The coordinates (x'_0, x', y') in such a frame are given by

$$\begin{pmatrix} x'_0 \\ x' \end{pmatrix} = \begin{pmatrix} \cosh q & -\sinh q \\ -\sinh q & \cosh q \end{pmatrix} \begin{pmatrix} x_0 \\ x \end{pmatrix}, \qquad y' = y,$$

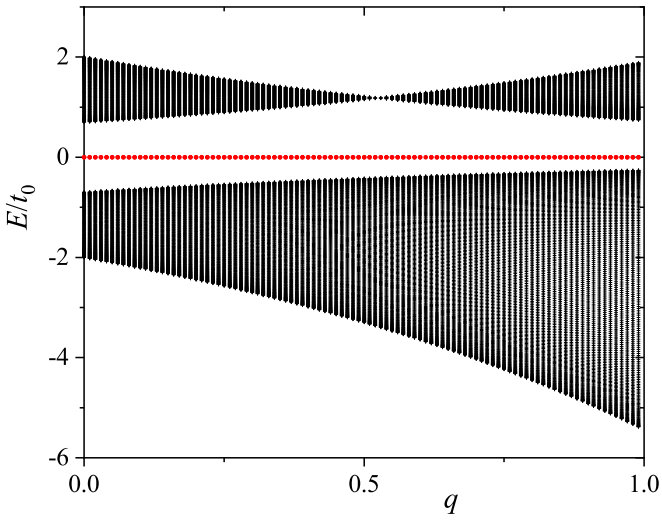

FIG. 6. Energy eigenvalues for a finite system with 200 unit cells having two open boundaries at each end of the system. The parameters are assumed to be $t/t_0 = 0.65$ and $t'/t_0 = 1.35$. The bulk states in the Bloch bands are plotted by black symbols while the two edge states at $E = 0$, located either the left or the right ends of the system, are plotted by red symbols.

where the parameter q is given by $\tanh q = \frac{v}{c}$ with the speed of light c. In this frame, the Schrödinger equation becomes

$$\exp(q\sigma_x/2)[\partial'_0 + \sigma_x\partial'_x + \sigma_y\partial'_y]\exp(q\sigma_x/2)\psi = 0,$$

with which we arrive at $[\partial'_0 + \sigma_x\partial'_x + \sigma_y\partial'_y]\psi' = 0$ with $\psi' = e^{q\sigma_x/2}\psi$, where $\partial'_0 = \frac{\partial}{\partial x'_0}$, $\partial'_x = \frac{\partial}{\partial x'}$, and $\partial'_y = \frac{\partial}{\partial y'}$. The present deformation for the operator $[\partial_0 + \sigma_x\partial_x + \sigma_y\partial_y]$ therefore corresponds to the Lorentz boost with $\tanh q = v/c$.

APPENDIX B: WINDING NUMBER OF DEFORMED SYSTEMS

Here we consider the deformation

$$H_\tau(q) = T_\tau(q)^{-1} H_{\rm SSH} T_\tau(q)^{-1},$$

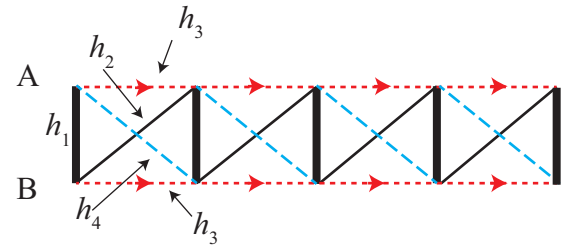

FIG. 7. The SSH model deformed by σ_y in real space. Thick solid lines (black), thin solid lines (black), dotted lines (red), and dashed lines (blue) represent hopping amplitudes h_1, h_2, h_3, and h_4, respectively. The hopping h_3 becomes imaginary while the others are real.

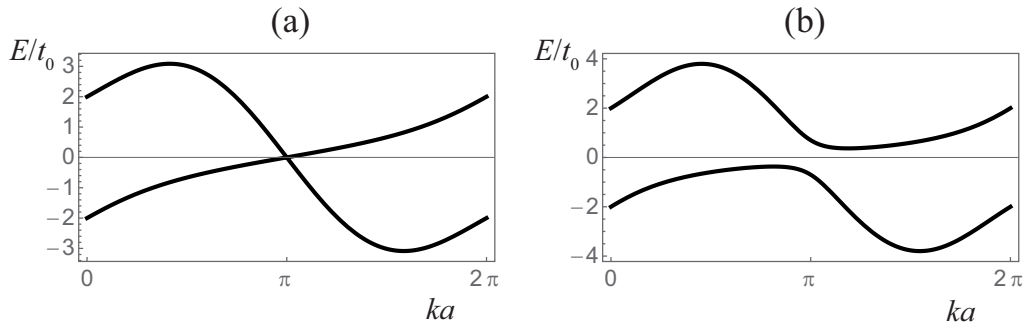

FIG. 8. Examples of the energy dispersion $E^{\hat{y}}_{q,\pm}(k)$ for $q = 1.0$. The critical case (a) $t/t' = 1.0$ and the topological cases (b) $t/t_0 = 0.65$ and $t'/t_0 = 1.35$ are presented. Although the time-reversal symmetry is broken, we have a relation $E^{\hat{y}}_{q,\pm}(k) = E^{\hat{y}}_{-q,\pm}(-k) = E^{\hat{y}}_{q,\mp}(-k)$.

with $\boldsymbol{\tau} = (\cos\theta, \sin\theta, 0)$, which yields in the momentum space

$$H_\tau(q) = -\sinh q\,\mathrm{Re}[e^{i\theta}d(k)]I_2 + \begin{pmatrix} 0 & d_{q,\theta}(k) \\ d^*_{q,\theta}(k) & 0 \end{pmatrix},$$

where $d_{q,\theta}(k) = e^{-i\theta}\{\mathrm{Re}[e^{i\theta}d(k)]\cosh q + i\,\mathrm{Im}[e^{i\theta}d(k)]\}$ with $d(k) = t + t'e^{-ik}$ and I_2 stands for the 2×2 identity matrix. The energy eigenvalues are given by

$$E^\tau_{q,\pm} = -\sinh q\,\mathrm{Re}[e^{i\theta}d(k)] \pm \sqrt{|d_{q,\theta}(k)|^2},$$

and the corresponding eigenstates $|\psi^\tau_\pm\rangle$ with $H_\tau(q)|\psi^\tau_\pm\rangle = E^\tau_{q,\pm}|\psi^\tau_\pm\rangle$ are given by

$$|\psi^\tau_\pm\rangle = \frac{1}{\sqrt{2}}\begin{pmatrix} \pm\alpha^*_\tau \\ 1 \end{pmatrix}, \quad \alpha^*_\tau = \frac{d_{q,\theta}(k)}{|d_{q,\theta}(k)|}.$$

The Q matrix [7] is therefore given by

$$Q = |\psi^\tau_+\rangle\langle\psi^\tau_+| - |\psi^\tau_-\rangle\langle\psi^\tau_-| = \begin{pmatrix} 0 & \alpha^*_\tau \\ \alpha_\tau & 0 \end{pmatrix}.$$

The winding number w can then be defined by

$$w = \frac{i}{2\pi}\int_{\mathrm{BZ}} d\alpha_\tau\,\alpha_\tau^{-1}.$$

This winding number becomes nonzero when the trajectory of $d_{q,\theta}(k)$ in the complex plane encircles the origin when k moves from 0 to 2π. For $q = 0$, $d_{q,\theta}(k)$ becomes $d(k)$ and it encircles the origin when $t' > t$ [7,8]. In the present deformed systems with $q \neq 0$, $d_{q,\theta}(k)$ is simply scaled by a factor $\cosh q$ in the direction determined by θ and hence the winding number is the same as $d(k)$. The winding number is therefore an invariant of the present deformation, with which we conclude that the topological phase in the deformed systems is always given by $t' > t$ and the bulk-edge correspondence is valid independent of q.

APPENDIX C: DEFORMED SSH MODELS WITH/WITHOUT TIME-REVERSAL SYMMETRY

Here we show typical cases of deformed SSH models with/without the time-reversal symmetry. When we assume $\boldsymbol{\tau} = \hat{\boldsymbol{x}} = (1, 0, 0)$, the deformed SSH model

$$H_{\hat{x}}(q) = \exp(-q\sigma_x/2)H_{\mathrm{SSH}}\exp(-q\sigma_x/2)$$

respects the time-reversal symmetry. In this case, a next-nearest neighbor and a third-nearest neighbor transfer integrals as well as a uniform energy shift emerge in the deformed Hamiltonian in the real space, which is equivalent to a ladder Hamiltonian described by

$$H^{\hat{x}}_q = \sum_n \varepsilon(a^\dagger_n a_n + b^\dagger_n b_n) + \sum_n t_1 a^\dagger_n b_n + t_2 a^\dagger_{n+1} b_n + t_3(a^\dagger_{n+1}a_n + b^\dagger_{n+1}b_n) + t_4 a^\dagger_{n-1}b_n + \mathrm{H.c.},$$

where $\varepsilon = -t\,\sinh q$, $t_1 = t\,\cosh q$, $t_2 = t'(\cosh q + 1)/2$, $t_3 = -t'(\sinh q)/2$, and $t_4 = t'(\cosh q - 1)/2$ (Fig. 4).

In this series of deformed topological SSH models, we find at $q = \tanh^{-1}(t/t')$ that the deformed model has a flatband. Note that this flatband model appears only when the original SSH model is topologically nontrivial ($t' > t$). In fact, for the case $\tanh q = t/t'$, we have

$$E^{\hat{x}}_{q,+} = \sqrt{t'^2 - t^2}, \qquad E^{\hat{x}}_{q,-} = \frac{-(t'^2 + t^2) - 2tt'\cos k}{\sqrt{t'^2 - t^2}},$$

and hence the energy of the flatband is $\sqrt{t'^2 - t^2}$. In Fig. 5, we show examples of the energy dispersions of the deformed SSH

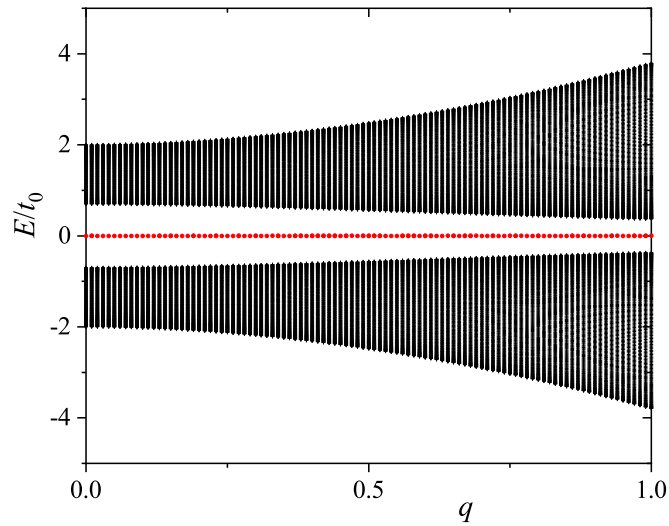

FIG. 9. Energy eigenvalues for a finite system with 200 unit cells having two open boundaries at each end of the system. The parameters are assumed to be $t/t_0 = 0.65$ and $t'/t_0 = 1.35$. The bulk states in the Bloch bands are plotted by black symbols while the two edge states at $E = 0$ are plotted by red symbols.

model, where the energy bands become asymmetric for $q \neq 0$. Models generated by the present deformation are, however, topologically nontrivial for any q. The energy gap, which can be indirect [Fig. 5(d)], never closes in the deformation.

The bulk-edge correspondence in the present models can be confirmed by the appearance of the edge states when the system has open boundaries. We show in Fig. 6 the energy eigenvalues of a finite system with open boundaries at each end of the system. It is clearly seen that the edge states exist exactly at zero energy throughout the deformation.

Next, we consider the models with $\boldsymbol{\tau} = \hat{\boldsymbol{y}} = (0, 1, 0)$ as

$$H_{\hat{y}}(q) = \exp(-q\sigma_y/2) H_{\mathrm{SSH}} \exp(-q\sigma_y/2),$$

where the time-reversal invariance is broken for $q \neq 0$. In the real space, the Hamiltonian can be written again in a ladder system as (Fig. 7)

$$H_q^{\hat{y}} = \sum_n h_1 a_n^\dagger b_n + h_2 a_{n+1}^\dagger b_n + h_3 (a_{n+1}^\dagger a_n + b_{n+1}^\dagger b_n) + h_4 a_{n-1}^\dagger b_n + \mathrm{H.c.},$$

where $h_1 = t$, $h_2 = t'(\cosh q + 1)/2$, $h_3 = -it'(\sinh q)/2$, and $h_4 = -t'(\cosh q - 1)/2$. Because of the breaking of the time-reversal invariance, the hopping t_3' becomes imaginary.

Examples of the dispersion relations for the deformed systems are shown in Fig. 8, where $E_{q,\pm}^{\hat{y}}(k) \neq E_{q,\pm}^{\hat{y}}(-k)$ due to the breaking of the time-reversal invariance.

The appearance of the edge states at $E = 0$ for an open system is also confirmed for $t' > t$. In Fig. 9, we show the energy eigenvalues of an open system with 200 unit cells, where the spectra are symmetric with respect to $E = 0$. The edge states at $E = 0$ again exist for any value of q.

[1] M. Z. Hasan and C. L. Kane, Rev. Mod. Phys. **82**, 3045 (2010).
[2] X.-L. Qi and S.-C. Zhang, Rev. Mod. Phys. **83**, 1057 (2011).
[3] Y. Hatsugai, Phys. Rev. Lett. **71**, 3697 (1993).
[4] A. Altland and M. R. Zirnbauer, Phys. Rev. B **55**, 1142 (1997).
[5] S. Ryu, A. P. Schnyder, A. Furusaki, and A. W. W. Ludwig, New J. Phys. **12**, 065010 (2010).
[6] Y. Hatsugai and H. Aoki, in *Physics of Graphene*, edited by H. Aoki and M. S. Dresselhaus (Springer, Heidelberg, New York, 2014), p. 213.
[7] C.-K. Chiu, J. C. Y. Teo, A. P. Schnyder, and S. Ryu, Rev. Mod. Phys. **88**, 035005 (2016).
[8] S. Ryu and Y. Hatsugai, Phys. Rev. Lett. **89**, 077002 (2002).
[9] S. Yao and Z. Wang, Phys. Rev. Lett. **121**, 086803 (2018).
[10] K. Yokomizo and S. Murakami, Phys. Rev. Lett. **123**, 066404 (2019).
[11] T. Kawarabayashi, Y. Hatsugai, T. Morimoto, and H. Aoki, Phys. Rev. B **83**, 153414 (2011); Int. J. Mod. Phys.: Conf. Ser. **11**, 145 (2012).
[12] Y. Hatsugai, T. Kawarabayashi, and H. Aoki, Phys. Rev. B **91**, 085112 (2015).
[13] T. Kawarabayashi, H. Aoki, and Y. Hatsugai, Phys. Rev. B **94**, 235307 (2016).
[14] N. Tajima, S. Sugawara, M. Tamura, Y. Nishio, and K. Kajita, J. Phys. Soc. Jpn. **75**, 051010 (2006).
[15] S. Katayama, A. Kobayashi, and Y. Suzumura, J. Phys. Soc. Jpn. **75**, 054705 (2006); **75**, 023708 (2006).
[16] A. Kobayashi, S. Katayama, Y. Suzumura, and H. Fukuyama, J. Phys. Soc. Jpn. **76**, 034711 (2007).
[17] A. Kobayashi, Y. Suzumura, H. Fukuyama, and M. O. Goerbig, J. Phys. Soc. Jpn. **78**, 114711 (2009).
[18] K. Kajita, Y. Nishio, N. Tajima, Y. Suzumura, and A. Kobayashi, J. Phys. Soc. Jpn. **83**, 072002 (2014).
[19] M. O. Goerbig, J.-N. Fuchs, G. Montambaux, and F. Piéchon, Phys. Rev. B **78**, 045415 (2008).
[20] T. Morinari, T. Himura, and T. Tohyama, J. Phys. Soc. Jpn. **78**, 023704 (2009).
[21] H. B. Nielsen and M. Ninomiya, Nucl. Phys. B **185**, 20 (1981).
[22] Y. Hatsugai, T. Fukui, and H. Aoki, Phys. Rev. B **74**, 205414 (2006); Eur. Phys. J.: Spec. Top. **148**, 133 (2007).
[23] Y. Hatsugai, J. Phys.: Conf. Ser. **334**, 012004 (2011).
[24] T. Kawarabayashi, H. Aoki, and Y. Hatsugai, Phys. Status Solidi B **256**, 1800524 (2019).
[25] W. P. Su, J. R. Schrieffer, and A. J. Heeger, Phys. Rev. Lett. **42**, 1698 (1979); Phys. Rev. B **22**, 2099 (1980).
[26] R. Jackiw and C. Rebbi, Phys. Rev. D **13**, 3398 (1976).
[27] W. P. Su and J. R. Schrieffer, Phys. Rev. Lett. **46**, 738 (1981).
[28] J. Goldstone and F. Wilczek, Phys. Rev. Lett. **47**, 986 (1981).
[29] M. J. Rice and E. J. Mele, Phys. Rev. Lett. **49**, 1455 (1982).
[30] R. Jackiw and G. Semenoff, Phys. Rev. Lett. **50**, 439 (1983).
[31] A. J. Heeger, S. Kivelson, J. R. Schrieffer, and W. P. Su, Rev. Mod. Phys. **60**, 781 (1988).
[32] E. J. Meier, F. A. An, and B. Gadway, Nat. Commun. **7**, 13986 (2016); Phys. Rev A **93**, 051602(R) (2016).
[33] R. Drost, T. Ojanen, A. Harju, and P. Liljeroth, Nat. Phys. **13**, 668 (2017).
[34] M. N. Huda, S. Kezilebieke, T. Ojanen, R. Drost, and P. Liljeroth, Quantum Mater. **5**, 17 (2020).
[35] K. Hashimoto, T. Kimura, and X. Wu, Prog. Theor. Exp. Phys. **2017**, 053I01 (2017); **2019**, 029201 (2019).
[36] C. Tauber, P. Delplace, and A. Venaille, Phys. Rev. Res. **2**, 013147 (2020).
[37] D. R. Candido, M. Kharitonov, J. C. Egues, and E. M. Hankiewicz, Phys. Rev. B **98**, 161111(R) (2018).
[38] V. Lukose, R. Shankar, and G. Baskaran, Phys. Rev. Lett. **98**, 116802 (2007).
[39] S. Tchoumakov, M. Civelli, and M. O. Goerbig, Phys. Rev. B **95**, 125306 (2017).
[40] S. Tchoumakov, V. Jouffrey, A. Inhofer, E. Bocquillon, B. Plaçais, D. Carpentier, and M. O. Goerbig, Phys. Rev. B **96**, 201302(R) (2017).
[41] A. Inhofer, S. Tchoumakov, B. A. Assaf, G. Fève, J. M. Berroir, V. Jouffrey, D. Carpentier, M. O. Goerbig, B. Plaçais, K. Bendias, D. M. Mahler, E. Bocquillon, R. Schlereth, C. Brüne, H. Buhmann, and L. W. Molenkamp, Phys. Rev. B **96**, 195104 (2017).